ORIGINAL ARTICLE

In vivo MR study of neuro-glial hippocampal changes in a rat model of fractionated craniospinal irradiation

Petra Hnilicová [1], **Soňa Bálentová** [2], **Dagmar Kalenská** [3], **Peter Muríň** [5], **Eva Hajtmanová** [5], **Dušan Dobrota** [4], **Ján Lehotský** [1,4]

[1] Biomedical Center Martin – Division of Neurosciences, [2] Department of Histology and Embryology, [3] Department of Anatomy and [4] Department of Medical Biochemistry, Jessenius Faculty of Medicine in Martin, Comenius University in Bratislava, Martin, Slovakia; [5] Department of Radiotherapy and Oncology, Martin University Hospital, Martin, Slovakia.

Correspondence to: Ing. Petra Hnilicová, PhD., Biomedical Center Martin – Division of Neurosciences, Jessenius Faculty of Medicine in Martin, Comenius University in Bratislava, Malá Hora 4D, 036 01 Martin, Slovakia.
TEL: +421-43-2633-660; E-MAIL: petra.hnilicova@uniba.sk

Abstract

OBJECTIVES: There are known several radiation-induced metabolic and histopathological changes in the brain that limit the treatment strategies in clinical radiotherapy. Although animal models enable to imitate irradiated injury, it is only poorly explored the early response of the brain to a clinically relevant fractionated irradiation.
METHODS: The aim of this experimental (8 irradiated and 5 sham-irradiated 3 months old Wistar male rats) *in vivo* MR study performed on 7T Bruker MR-scanner was to investigate volumetric atrophy and metabolic changes in the dorsal hippocampus induced early (18–21 weeks) after the fractionated craniospinal irradiation (35 Gy in 7 fractions).
RESULTS: Outcomes in this study indicate high neurodegeneration (decreased N-acetyl aspartate to creatine ratio) accompanied with demyelinated processes (increased choline-containing compounds to creatine ratio) and reactive astrogliosis (increased myo-Inositol ratios) in dorsal hippocampus of exposed animals. Metabolic changes were closely associated with MR-observable hippocampal atrophy, as well as with increasing neurodegeneration confirmed by Fluoro-Jade C+ cell detection in hippocampal dentate gyrus of irradiated animals.
CONCLUSION: Results of this *in vivo* MR study showed structural, metabolic and histological alterations suggesting a subacute development of early radiation-induced changes after clinically relevant fractionated craniospinal irradiation.

INTRODUCTION

Radiation-induced brain injury usually occurs after conventional radiation therapy of patients with primary brain tumors and metastases and is caused by microstructural and/or metabolic changes in neural tissue (Wong & Van der Kogel 2004; Yang *et al* 2015).

Based on the clinical persistence and relevance, radiation-induced brain injury is described as acute, early-delayed and late injury (Kaminaga & Shirai 2005; Chan *et al* 2009). It is becoming evident that although fractionated ionizing radiation is applied, it still influences neuronal, glial, and endothelial cell population in the brain (Wong & Van der Kogel 2004; Greene-

Petra Hnilicová, Soňa Bálentová, Dagmar Kalenská, Peter Murín, Eva Hajtmanová, Dušan Dobrota, Ján Lehotský

Schloesser *et al* 2012). Radiation-induced changes develop slowly, but their histopathological and functional deficits are irreversible and significantly impair the quality of life (Lledo *et al* 2006; Yang *et al* 2015). From clinical radiotherapy are known several post-radiation mechanisms like progressive neurodegeneration, disrupted neurogenesis, ongoing demyelination, and white matter necrosis, as well as functional consequences of irradiation, especially progressive cognitive impairment (Podo *et al* 2011; Greene-Schloesser *et al* 2012; Makale *et al* 2017). Considering the spatial restriction of neurogenesis and learning/memory-controlling cognitive brain centers, among the most affected specific brain regions belongs hippocampus (Kempermann 2002; Lledo *et al* 2006). Although animal models enable to imitate mechanisms of irradiated injury, it is only poorly explored the brain tissue response to a clinically relevant fractionated irradiation (Yang *et al* 2015; Brown *et al* 2016). Therefore, the aim of this advanced *in vivo* MR study was to investigate neuro-glial hippocampal changes induced early (18–21 weeks survival time) after the fractionated craniospinal irradiation (total dose of 35 Gy) equivalent to the treatment dose used in many tumor modalities (Wong & Van der Kogel 2004; Fowler 2010). Based on *in vivo* magnetic resonance (MR) volumetry and proton magnetic resonance spectroscopy (^{1}H MRS) were examined volumetric atrophy and metabolic changes in the dorsal hippocampus to establish the relationship with histochemical alterations revealed by Fluoro-Jade C+ cell detection in hippocampal dentate gyrus of exposed experimental animals.

MATERIALS AND METHODS

Animal experiments in this study were approved by the Animal Care and Use Committee, Jessenius Faculty of Medicine in Martin, Comenius University in Bratislava, Slovak Republic (no. 4204/14-221). Fourteen Wistar male rats (Velaz, Prague, Czech Republic) 3–4 months old at the start of the study and weighing approximately 300–400 g were used in this study. Animals were maintained in s climate-controlled rooms (temperature of 22±2 °C, relative humidity 55±10 %) in a light-controlled conditions (12/12 h light/dark cycle) and provided with food and water *ad libitum*.

Induction of the craniospinal irradiation
Craniospinal irradiation was delivered to anesthetized rats (i.p. ketamine hydrochloride of a dose of 1–2 ml/kg body weight and s.c. xylazine hydrochloride of a dose of 0.1–0.2 ml/kg body weight) by Teragam KO-2 device (UJP, Prague, Czech Republic) using the radioactive isotope ^{60}Co with the energy of 1.17 and 1.33 MeV. Fractionated irradiation with a biological effective dose (BED) of 117 Gy was delivered in 5 Gy per fraction during 7 consecutive weeks (total dose of 35 Gy). Early (18–21 weeks) after the irradiation procedures irradi-ated (IRR; n=8) and sham irradiated (SHAM; n=5) animals underwent in vivo magnetic resonance (MR) examinations. After MR experiments, histochemical analysis were performed on brain samples.

MR examinations
In vivo MR measurements were performed on 7T small animal MR scanner Bruker BioSpec 70/20 USR (Bruker BioSpin, Ettlingen, Germany) using a combination of the proton (^{1}H) volume resonator and the 4-elements ^{1}H surface array coil (Bruker BioSpin, Ettlingen, Germany). During the whole scanning procedure (in total ~40 min) were animals anesthetized (sevoflurane in medical oxygen: 6% and 3.5–4.5% for anesthetic induction and maintenance), stabilized with tooth holder and nose mask in a dedicated water heated bed (Bruker BioSpin MRI), and monitored (rectal temperature, respiratory rate). To ensure similar brain regions positioning, three-dimensional T_2-weighted MR images (MRI) in tree orthogonal directions were measured (RARE – rapid acquisition with relaxation enhancement; TR (repetition time)/ TE (echo time) = 2680/40 ms, 2 averages, image size = 256×256, FOV (field of view) = 35×35 mm^2, resolution 0.137×0.137×0.5 mm^3, 23 slices with 0.5 mm slice thickness and 0.3 mm gap, ~2 min acquisition time). For identify magnetic field (B_0) inhomogeneity across the brain, B_0 phase map was obtained prior to proton magnetic resonance spectroscopy (^{1}H MRS) acquisitions. Subsequently, spectroscopic and shimming volumes were manually localized outside of B_0 distortions visible on the B_0 map. Spectroscopic data from dorsal hippocampus (DG, CA_{1-3}) were obtained using the two-dimensional chemical shift imaging (CSI) with following parameters: PRESS – Point RESolved Spectroscopy, TR/TE = 1500/20 ms, 36 averages, 8×8 CSI matrix with nominal voxel size of 8×10×1.6 mm^3, FOV = 22×22 mm^2; ~16 min acquisition time (Figure 1). During data acquisition, eddy currents and B_0 drift compensations, outer volume suppression and VAPOR-water suppression were applied. Linear and second order shims were automatically adjusted with the cuboid shim volumes, reaching the full width at half maximum (FWHM) of the water peak of 20–25 Hz. Spectroscopic data curve fitting and quantification of metabolite levels (tNAA, N-acetyl aspartate & N-acetyl aspartyl glutamate; tCr, creatine & phosphocreatine; tCho, choline & phosphocholine; mIns (myo-Inositol) were performed by LCModel software (version 6.3-1K; S. Provencher, Ontario, Canada). Spectra were accepted if the Full Width Half Maximum (FWHM) was <0.1 ppm and the signal-to-noise ratio (SNR) was >5. Finally were evaluated followed metabolite ratios: tNAA/tCr, tCr/tNAA, tCho/tCr, tCho/tNAA, mIns/tCr, and mIns/tNAA. Tissue volumetry was obtained using the semiautomatic ITK-SNAP software (Version 3.4.0, US National Institutes of Health, USA). The analyzed region of dorsal hippocampus was manually

outlined on consecutive coronal T_2-weighted MRI slices (Figure 2), for which the volume was automatically calculated by the software. Statistical analysis of differences in metabolite ratios and selected volume between IRR and SHAM animal groups was performed by sample independent two-tailed t-test using the SPSS software package (Version 15.0; Chicago, IL, USA).

Tissue processing and histochemistry
Following the anesthesia (6% sevoflurane in medical oxygen), IRR (n=8) and SHAM (n=5) animals were subjected to transcardial perfusion with saline and 4% paraformaldehyde in 0.1 M phosphate buffer (PB). Brains were after decapitation immersed overnight in the same fixative at 4 ºC and placed in 30% sucrose for 18h. Hemisected samples were covered with embedding medium (Killik, Bio Optica, Milano, Italy), frozen by rapid cooling boost in a cryobar (Shannon Cryotome E, Thermo Scientific Waltham, MA, USA) and cut in sagittal 30 µm frozen sections, collected on lysine-coated slides and air-dried. For Fluoro-Jade C histochemistry, the brain slides were oven dried (30 min at 55°C), rinsed (100% ethanol for 3 min, 70% ethanol for 2 min, distilled water for 1 min), incubated (0.06% potassium permanganate solution for 15 min followed for 1 min in distilled water), and transferred for 2h to a 0.0001% solution of Fluoro-Jade C dye (Millipore, Billerica, MA, USA) dissolved in 0.1% acetic acid vehicle. After rinsing through three changes of distilled water (for 1min per change), the air-dried slides were coverslipped with Fluoromount (Serva, Heidelberg, Germany). Fluoro-Jade-C immunoreactivity in the DG of hippocampus of each animal were captured with confocal laser scanning microscope OLYMPUS Fluoview FV10i (objective of 10× with zoom up to 20×), evaluated in Olympus Fluoview FV10-ASW software (version 02.01, Olympus Europa Holding GmbH, HAMBURG, Germany), and further processed in Adobe Photoshop CS3 Extended (version 10.0 for Windows, Adobe Systems, San Jose, CA, USA). Particle analysis in DG of hippocampus in all sections per animal were counted using ImageJ software (National Institute of Health, Bethesda, MD, USA). All counts of Fluoro-Jade C-positive (green fluorescent cytoplasm) cells were expressed as the total numbers of labelled cells per cm^2. Data obtained from image analysis of brain sections were analyzed in the SPSS software package (Version 15.0; Chicago, IL, USA) using the sample independent two-tailed t-test.
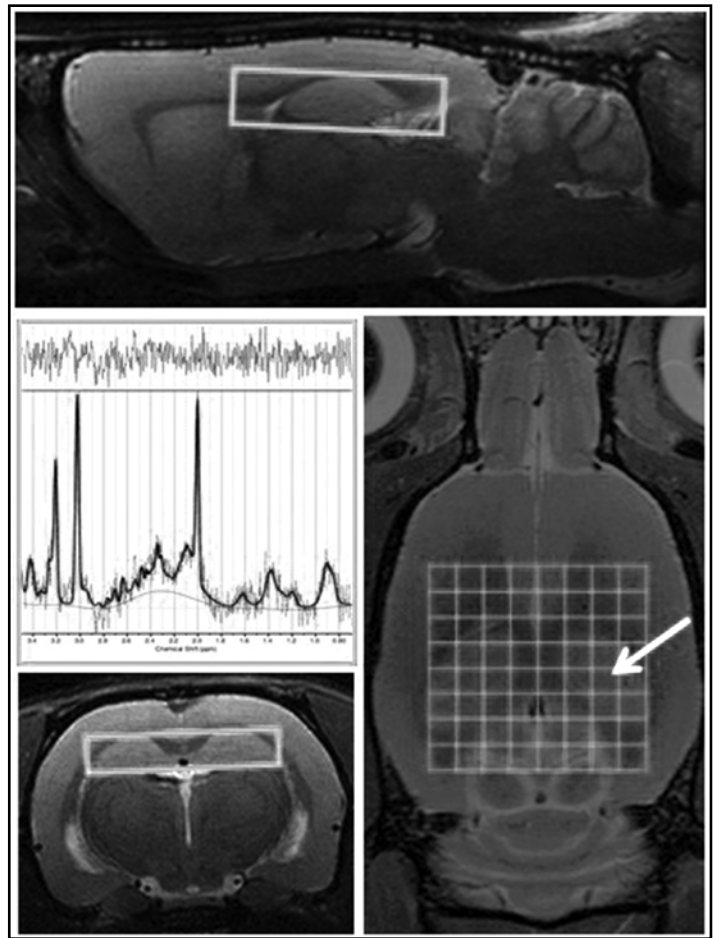

Fig. 1. Representative ^{1}H MRS in the dorsal hippocampus of irradiated animals. On morphological T_2-weighted MRI is displayed position of a ^{1}H MRS – 2D CSI 8×8 grid with the FOV of 22×22 mm^2 and nominal voxel size of 8×10×1.6 mm^3. Shown is also a representative ^{1}H MRS spectra obtained with the CSI technique in the dorsal hippocampus of experimental animals.
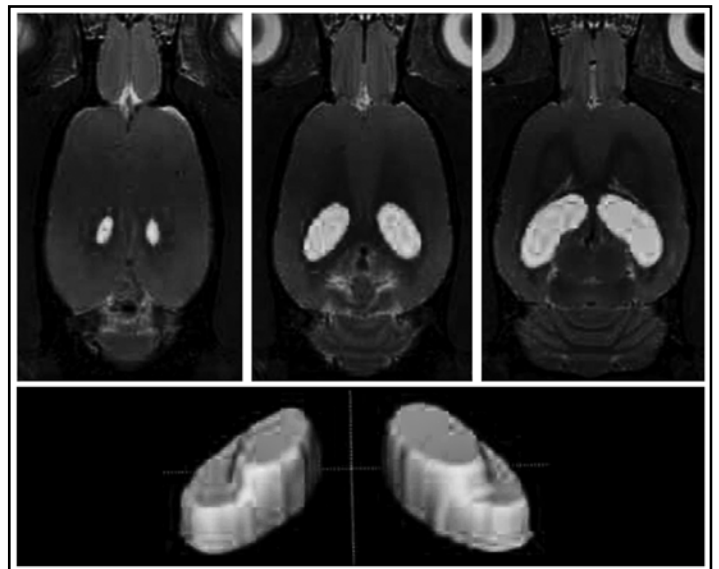

Fig. 2. Evaluation of MR-volumetry in dorsal hippocampus of experimental animals. On consecutive coronal T_2-weighted MRI with resolution of 0.137×0.137×0.5 mm^3 is displayed representative ROIs covering dorsal hippocampus together with 3D visualization of target areas plotted by ITK-SNAP software (Version 3.4.0, US National Institutes of Health, USA).

Results

In this study we did not observe relevant changes in the body weight between SHAM and IRR rats (SHAM: 475.40 ± 17.40 g versus IRR: 428.43 ± 15.36 g), even not in the irradiated group at the beginning and at the end of the study (beginning: 409.67 ± 6.95 g versus end: 428.43 ± 15.36 g). We did not measure the mean brain weight, because the tissue can be altered by infusion of fixative fluid. However, volumes of dorsal hippocampus were evaluated based on *in vivo* MRI volumetric measurement. Furthermore, in this study were corre-lated results of ^{1}H MRS metabolic changes and histo-chemical Fluoro-Jade C$^+$ cells degradations in dorsal hippocampus.

MR volumetric and ^{1}H MRS metabolic changes in hippocampus

In this study, significantly decreased tNAA/tCr ($p=0.002$) and increased tCr/tNAA ($p=0.004$) meta-bolic ratios were found in dorsal hippocampus of IRR animals compare to SHAM group (Table 1). Further-more, in IRR animals were observed significant eleva-tion of both mIns metabolic ratios (mIns/tCr: $p=0.015$, mIns/tNAA: $p=0.001$) and tCho/tNAA ($p=0.038$), how-ever in tCho/tCr were no significant changes ($p=0.742$). MR volumetric analysis showed a significant atrophy of dorsal hippocampus ($p=0.013$) in IRR compare to SHAM group (Table 1).

Fluoro-Jade C positivity in hippocampus

To display the extent of neuronal degeneration, we used Fluoro-Jade C$^+$ to detect the disintegrated neurons in tissue slices of the DG area of hippocampus in rats (Figure 3). The Fluoro-Jade dye is a high affinity fluo-rescent marker, which stains somas, dendrites, axons, and axon terminals of degenerating neurons, but is not expressed in intact nervous tissue. In this study, signifi-cantly increased Fluoro-Jade C$^+$ neurons were found in the hippocampal DG of IRR compared to SHAM animal group (IRR: 96 ± 7.83/cm^2 versus SHAM: no cells).

Discussion

Ionizing radiation influences neuronal, glial, and endo-thelial cell population in the brain and lead to significant metabolic, histopathological and functional deficits
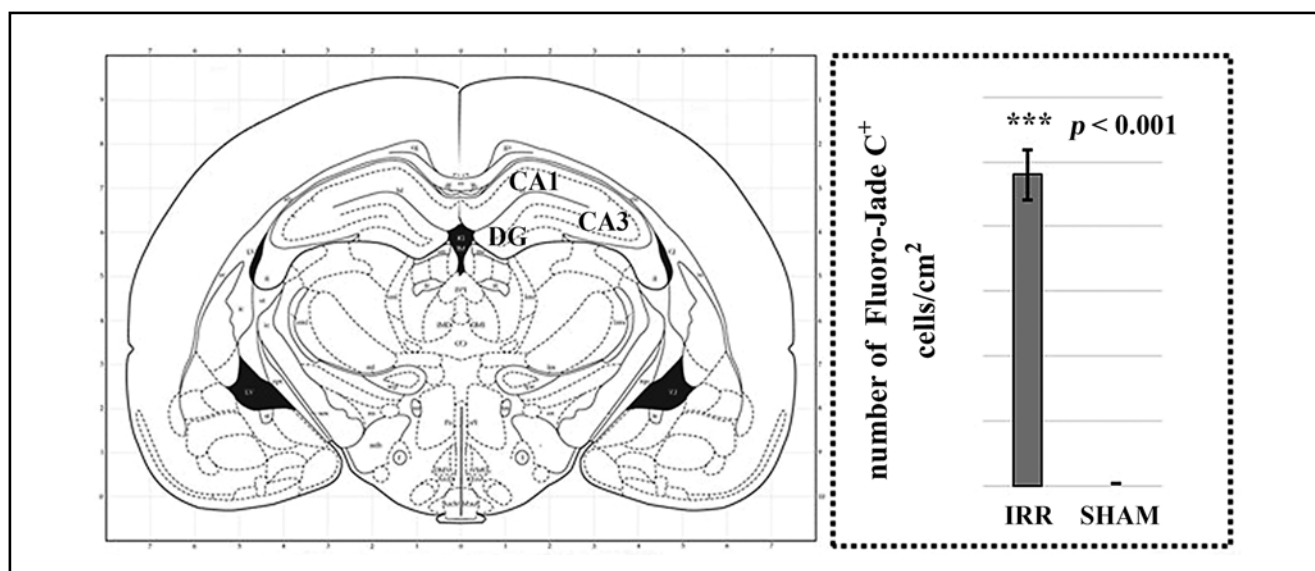
Tab. 1. Hippocampal metabolite ratios and volumetric values in experimental animals.

Metabolic ratios	DORSAL HIPPOCAMPUS		
	IRR (n=8) mean ± SD	SHAM (n=5) mean ± SD	*p*-values
tNAA/tCr	0.782 ± 0.097	1.006 ± 0.103	0.002
tCr/tNAA	1.296 ± 0.159	1.003 ± 0.108	0.004
tCho/tCr	0.249 ± 0.058	0.239 ± 0.037	0.742
tCho/tNAA	0.321 ± 0.071	0.239 ± 0.038	0.038
mIns/tCr	0.826 ± 0.209	0.528 ± 0.117	0.015
mIns/tNAA	1.058 ± 0.235	0.252 ± 0.095	0.001
volume [mm³]	38.6 ± 4.3	44.7 ± 4.2	0.013

Relative concentrations of metabolite ratios and tissue MRI volumes (mean ± SD) measured in dorsal hippocampus of IRR (n=8) and SHAM (n=5) animals using *in vivo* ^{1}H MRS at 7T Bruker MR-scanner. The *p*-values expressing statistical differences in metabolite ratios as well as in tissue MRI volumes between IRR and SHAM group performed by sample independent two-tailed t-test using the SPSS software package (Version 15.0; Chicago, IL, USA).

Fig. 3. Evaluation of Fluoro-Jade C$^+$ cells in hippocampus of experimental animals. Statistical evaluation of the number of Fluoro-Jade C$^+$ degenerating and dying neurons (means ± SD) in the DG of hippocampus (graphical depiction at the morphological brain scheme according to http://labs.gaidi.ca/rat-brain-atlas/) in theIRR animals, compare to intact nervous tissue in SHAM group.

(Wong & Van der Kogel 2004; Greene-Schloesser *et al* 2012). The most affected post-radiation mechanism is neurogenesis that is spatially restricted into the specific brain regions, predominantly in hippocampal dentate gyrus (Kempermann 2002; Lledo *et al* 2006). In this experimental *in vivo* MR-study of the early radiation-induced metabolic changes (18–21 weeks survival time after fractionated craniospinal irradiation in total dose of 35 Gy) in dorsal hippocampus we observed a significantly decreased tNAA/tCr together with increased tCr/tNAA metabolic ratio in exposed animals compare to control group. The nervous system-specific metabolite N-acetyl aspartate, which is the predominant component of tNAA complex, is synthesized from aspartate and acetyl-coenzyme A in neurons and transported to oligodendrocytes, where it serves as a source of acetyl groups for myelin lipid synthesis (Moffett *et al* 2007; Benarroch 2008; Barker *et al* 2009). It is also appears to adopt other roles, including a bioenergetics role in neuronal mitochondria, neuronal osmoregulation, axon-glial signaling, and function of a direct precursor for the brain most concentrated neuropeptide N-acetyl-aspartyl-glutamate (Moffett *et al* 2007; Soares & Law 2009). Therefore, the spectroscopic peak of tNAA is considered as a marker for the viability, functionality, and density of neurons (Benarroch 2008; Barker *et al* 2009). While the cerebral concentrations of tCr remain relatively constant, changes in tNAA/tCr or in tCr/tNAA ratios, reflect tNAA levels and in generally have been proved diagnostically important (Kornienko & Pronin 2009; Soares & Law 2009; Wijnen 2010). Decrease in tNAA signal is detected in damaged neurons (due to ischemia, sclerosis multiplex, Alzheimer diseases, epilepsy, etc.), or due to apoptosis and neuronal dysfunction secondary to irradiation (Soares & Law 2009; McKnight & Wladman 2010; Housni & Boujraf 2013). Although, only a few animal MR-studies are focused in radiation-induced metabolic changes in the brain tissue, they confirmed that irradiation with higher doses (27 Gy; 35 Gy; 45 Gy) and long-term survival (24 weeks; 48 weeks; 14 weeks) result in decrease in tNAA/tCr (Herynek *et al* 2004; Chan *et al* 2009; Brown *et al* 2016). Clinical outcomes also supported fact about decline of tNAA during acute, early as well as late post-treatment brain irradiation (Kaminaga & Shirai 2005; Balmaceda *et al* 2006; Podo *et al* 2011). Neurodegeneration was suggested in this study also based on a tissue atrophy evaluated by MRI-volumetry in dorsal hippocampus of exposed animals. However, the neuroimaging evidence of radiation-induced hippocampal changes are across preclinical and clinical studies different. In general, there is usually observed late-induced tissue atrophy (at least 6 months), but early occurred changes in neuro-axonal functions along with vascular damage and inflammation (Nolen *et al* 2016; Makale *et al* 2017; Seibert *et al* 2017). Hippocampus and associated limbic system have long been known to be important in learning and memory formation and therefore the radiation-induced injury of this brain area could lead to cognitive impairments (McKnight & Wladman 2010; Seibert *et al* 2017). In this study, observed metabolic changes in tNAA ratios as well as volumetric atrophy in dorsal hippocampus were closely associated with histochemical findings in irradiated animals, i.e. increasing neurodegeneration confirmed by Fluoro-Jade C+ cell detection in hippocampal DG. In general, studies focused in neurotoxic, ischemic, or another apoptotic cell death markers are in agreement that regard Fluoro-Jade C+ dyeing is a sensitive and unambiguous method for disturbed neural tissue identifying (Schmued *et al* 2005; Ehara & Ueda 2009). Several reports have demonstrated that Fluoro-Jade is also useful in detecting glia, specifically reactive astroglia and microglia (Schmued *et al* 2005; Damjanac *et al* 2007). Based on previous clinical and preclinical studies, irradiation cause reactive astrogliosis as well as microglial response at least 6 months after fractionated treatment (Yuan *et al* 2006; Greene-Schloesser *et al* 2012; Yang *et al* 2015). Regarding to observed hippocampal DG region, only our previous study was designed (20 Gy, 14 weeks survival time) to shown astrocytes activation in this region, revealing a lack of qualitative confirmation of astrogliosis after fractionated irradiation (Bálentová *et al* 2015). Microglial activation and myelinated tracts degradation with subsequent gliosis are associated with increased mIns, a MR-detectable marker of glial cellularity, especially of astrocytes (Barker *et al* 2009; Soares & Law 2009; Quarantelli 2015). In this light, results in this study indicate reactive astrogliosis (increased mIns ratios) with higher neurodegeneration (decreased tNAA/tCr) in dorsal hippocampus of exposed animals. Outcomes from previous animal studies are very inconsistent, revealed no changes, decrease, as well as increase in hippocampal mIns levels after single-dose (8 Gy in 10 days, 20 Gy in 14 weeks, and 28 Gy in 48 weeks survival) irradiation procedures (Chan *et al* 2009; Gupta *et al* 2013; Rodgers *et al* 2016). Reason may be the controversial function of astrocytes and microglia in the radiation-induced brain. They are accompanied by expression of pro- as well as anti-inflammatory cytokines and inflammatory mediators (Hwang *et al* 2006; Greene-Schloesser *et al* 2012; Quarantelli 2015). It is also known a dual role of astrocytes, which may contribute to oligodendrocytes degeneration and axons demyelination as well as create a permissive environment for remyelination (Soares & Law 2009; Greene-Schloesser *et al* 2012). Furthermore, tCho signals may suggest heightened cell-membrane turnover as seen in proliferative tissue, demyelination, remyelination, inflammation, and ongoing gliosis (Barker *et al* 2009; Housni & Boujraf 2013; Quarantelli 2015). Both, tCho/tNAA and tCho/tCr ratios, are considered as diagnostically beneficial, due to their correlation with degree of malignancy, but may reflect also the treatment efficiency, even prior to tumor atrophy occurred (Barker *et al* 2009; McKnight & Wladman 2010; Wijnen 2010). In this study, in dorsal hippocam-

Petra Hnilicová, Soňa Bálentová, Dagmar Kalenská, Peter Murín, Eva Hajtmanová, Dušan Dobrota, Ján Lehotský

pus of IRR animals was found increased tCho/tNAA, but tCho/tCr was not significantly elevated. Considering tCho as a membrane, tNAA as a neuronal, and tCr as a glial markers, the increased tCho/tNAA may show rather the intensive cell-membrane and myelin degradation correlating with high neurodegeneration than the increased gliosis in dorsal hippocampus of exposed animals (35 Gy) after the short (18–21 weeks) survival time. Similar outcomes are reported in previous experimental studies showing increased tCho in exposed animals with long-term (24 weeks and 27 Gy; 48 weeks and 28 Gy; 32 weeks and 35 Gy) survival times (Herynek *et al* 2004; Chan *et al* 2009; Brown *et al* 2016)s. As revealed in these outcomes, irradiation, even in early-delayed phase of treatment, had impact on neuronal functions and neurodegeneration, what support the suggestion of high neurotoxicity of fractionated irradiation with the high precautions also in human clinical conditions.

Conclusions

This study is one of only a few advanced *in vivo* MR studies examining the neuro-glial hippocampal changes in an experimental model of the therapeutically relevant fractionated craniospinal irradiation (total dose of 35 Gy) with early-delayed injury (18–21 weeks). Based on revealed outcomes, both neurodegenerative (decreased tNAA/tCr, increased tCr/tNAA) and inflammatory demyelinated processes (increased tCho/tCr) with reactive astrogliosis (increased mIns ratios) were observed in dorsal hippocampus of exposed animals, with predominant neurodegeneration in this brain area. As described above, metabolic changes of neuro-glial markers were closely associated with histochemical findings (i.e. increasing neurodegeneration confirmed by Fluoro-Jade C+ cell detection) as well as with volumetric atrophy in dorsal hippocampus of irradiated animals. This preclinical *in vivo* study revealed structural, metabolic and functional changes in the brain after therapeutically relevant fractionated craniospinal irradiation that may affect development of neural and cognitive deficits in human patients.

Acknowledgement

REFERENCES

1 Bálentová S, Hajtmanová E, Filová B, Borbelyová V, Lehotský J (2015) Effect of Fractionated Irradiation on the Hippocampus in an Experimental Model. *Klin Onkol*. **28**(3): 191–199.
2 Balmaceda C, Critchell D, Mao XL, Cheung K, Pannullo S, DeLaPaz RL, *et al* (2006) Multisection H-1 magnetic resonance spectroscopic imaging assessment of glioma response to chemotherapy. *J Neurooncol*. **76**(2): 185–191.
3 Barker P, Bizzi A, De Stefano N, Gullapalli R, Lin D (2009) Clinical MR Spectroscopy: Techniques and Applications. Cambridge: Cambridge University Press.
4 Benarroch EE (2008) N-Acetylaspartate and N-acetylaspartylglutamate – Neurobiology and clinical significance. *Neurology*. **70**(16): 1353–1357.
5 Brown RJ, Jun BJ, Cushman JD, Nguyen C, Beighley AH, Blanchard J, *et al* (2016) Changes in Imaging and Cognition in Juvenile Rats After Whole-Brain Irradiation. *Int J Radiat Oncol Biol Phys*. **96**(2): 470–478.
6 Damjanac M, Bilan AR, Barrier L, Pontcharraud R, Anne C, Hugon J, *et al* (2007) Fluoro-Jade (R) B staining as useful tool to identify activated microglia and astrocytes in a mouse transgenic model of Alzheimer's disease. *Brain Research*. **1128**(1): 40–49.
7 Ehara A, Ueda S (2009) Application of Fluoro-Jade C in Acute and Chronic Neurodegeneration Models: Utilities and Staining Differences. *Acta Histochem Cytochem*. **42**(6): 171–179.
8 Fowler JF (2010) 21 years of Biologically Effective Dose. *Br J Radiol*. **83**(991): 554–568.
9 Greene-Schloesser D, Robbins ME, Peiffer AM, Shaw EG, Wheeler KT, Chan MD (2012) Radiation-induced brain injury: a review. *Front Oncol*. **2**: 1–18.
10 Gupta M, Rana P, Trivedi R, Kumar BSH, Khan AR, Soni R, *et al* (2013) Comparative evaluation of brain neurometabolites and DTI indices following whole body and cranial irradiation: a magnetic resonance imaging and spectroscopy study. *NMR Biomed*. **26**(12): 1733–1741.
11 Herynek V, Burian M, Jirak D, Liscak R, Namestkova K, Hajek M, *et al* (2004) Metabolite and diffusion changes in the rat brain after Leksell Gamma Knife irradiation. *Magn Reson Med*. **52**(2): 397–402.
12 Housni A, Boujraf S (2013) Multimodal magnetic resonance imaging in the diagnosis and therapeutical follow-up of brain tumors. *Neurosciences*. **18**(1): 3–10.
13 Hwang SY, Jung JS, Kim TH, Lim SJ, Oh ES, Kim JY, *et al* (2006) Ionizing radiation induces astrocyte gliosis through microglia activation. *Neurobiol Dis*. **21**(3): 457–467.
14 Chan KC, Khong PL, Cheung MM, Wang SL, Cai KX, Wu EX (2009) MRI of Late Microstructural and Metabolic Alterations in Radiation-Induced Brain Injuries. *J Magn Reson Imaging*. **29**(5): 1013–1020.
15 Kaminaga T, Shirai K (2005) Radiation-induced brain metabolic changes in the acute and early delayed phase detected with quantitative proton magnetic resonance spectroscopy. *J Comput Assist Tomogr*. **29**(3): 293–297.
16 Kempermann G (2002) Why new neurons? Possible functions for adult hippocampal neurogenesis. *J Neurosci*. **22**(3): 635–638.
17 Kornienko VN, Pronin IN (2009) Diagnostic Neuroradiology. Berlin: Springer Berlin Heidelberg.
18 Lledo PM, Alonso M, Grubb MS (2006) Adult neurogenesis and functional plasticity in neuronal circuits. *Nat Rev Neurosci*. **7**(3): 179–193.
19 Makale MT, McDonald CR, Hattangadi-Gluth J, Kesari S (2017) Brain irradiation and long-term cognitive disability: Current concepts. *Nat Rev Neurol*. **13**(1): 52–64.
20 McKnight TR, Wladman AD (2010) Magnetic resonance spectroscopy in adult neoplasia. In: Gillard JH, Wladman AD and Barker PB. Clinical MR Neuroimaging. Cambridge University Press.
21 Moffett JR, Ross B, Arun P, Madhavarao CN, Namboodiri AMA (2007) N-acetylaspartate in the CNS: From neurodiagnostics to neurobiology. *Prog Neurobiol*. **81**(2): 89–131.
22 Nolen SC, Lee B, Shantharam S, Yu HJ, Su L, Billimek J, *et al* (2016) The effects of sequential treatments on hippocampal volumes in malignant glioma patients. *J Neurooncol*. **129**(3): 433–441.
23 Podo F, Canevari S, Canese R, Pisanu ME, Ricci A, Iorio E (2011) MR evaluation of response to targeted treatment in cancer cells. *NMR Biomed*. **24**(6): 648–672.
24 Quarantelli M (2015) MRI/MRS in neuroinflammation: methodology and applications. *Clin Transl Imaging*. **3**(6): 475–489.

25 Rodgers SP, Zawaski JA, Sahnoune I, Leasure JL, Gaber MW (2016) Radiation-Induced Growth Retardation and Microstructural and Metabolite Abnormalities in the Hippocampus. *Neural Plast*. **2016**.12pp.

26 Seibert TM, Karunamuni R, Bartsch H, Kaifi S, Krishnan AP, Dalia Y, *et al* (2017) Radiation Dose-Dependent Hippocampal Atrophy Detected With Longitudinal Volumetric Magnetic Resonance Imaging. *International Journal of Radiation Oncology Biology Physics*. **97**(2): 263–269.

27 Schmued LC, Stowers CC, Scallet AC, Xu LL (2005) Fluoro-Jade C results in ultra high resolution and contrast labeling of degenerating neurons. *Brain Research*. **1035**(1): 24–31.

28 Soares DP, Law M (2009) Magnetic resonance spectroscopy of the brain: review of metabolites and clinical applications. *Clin Radiol*. **64**(1): 12–21.

29 Wijnen JP (2010) Multi-nuclear Magnetic Resonance Spectroscopy of human brain tumours. GVO drukkers & vormgevers B.V.

30 Wong CS, Van der Kogel AJ (2004) Mechanisms of radiation injury to the central nervous system: implications for neuroprotection. *Molecular Interventions*. **4**(5): 273–284.

31 Yang Z, Bai S, Gu B, Peng S, Liao W, Liu J (2015) Radiation-Induced Brain Injury After Radiotherapy for Brain Tumor. In: Lichtor T. Molecular Considerations and Evolving Surgical Management Issues in the Treatment of Patients with a Brain Tumor. IntechOpen.

32 Yuan H, Gaber MW, Boyd K, Wilson CM, Kiani MF, Merchant TE (2006) Effects of fractionated radiation on the brain vasculature in a murine model: Blood-brain barrier permeability, astrocyte proliferation, and ultrastructural changes. *International Journal of Radiation Oncology Biology Physics*. **66**(3): 860–866.